Lyapunov timescales and black hole binaries

Neil J. Cornish* and Janna Levin**
* *Department of Physics, Montana State University, Bozeman, MT 59717*
** *DAMTP, Cambridge University,Wilberforce Rd., Cambridge CB3 0WA*

Black holes binaries support unstable orbits at very close separations. In the simplest case of geodesics around a Schwarzschild black hole the orbits, though unstable, are regular. Under perturbation the unstable orbits can become the locus of chaos. All unstable orbits, whether regular or chaotic, can be quantified by their Lyapunov exponents. The exponents are observationally relevant since the phase of gravitational waves can decohere in a Lyapunov time. If the timescale for dissipation due to gravitational waves is shorter than the Lyapunov time, chaos will be damped and essentially unobservable. We find the two timescales can be comparable. We emphasize that the Lyapunov exponents must only be used cautiously for several reasons: they are relative and depend on the coordinate system used, they vary from orbit to orbit, and finally they can be deceptively diluted by transient behaviour for orbits which pass in and out of unstable regions.

04.30.Db,97.60.Lf,97.60.Jd,95.30.Sf,04.70.Bw,05.45

Newtonian gravity predicts the elliptical planetary orbits around the sun which Kepler described. Einstein gravity predicts precessing elliptical orbits around a central star, thereby reconciling the precession of the perihelion of Mercury with general relativity. In the extreme case of a central black hole, there are also a simple set of *unstable* circular orbits in addition to the usual stable circular orbits. Related to these are the homoclinic orbits which lie on the boundary between dynamical stability and instability [1,2]. To the list of possible orbits, a set of chaotic orbits has recently been added for rapidly spinning black holes [3–5] (and for the interesting but less physically realistic Majumdar-Papapetrou black hole pairs of equal mass and charge [6–9]). With the future gravitational wave experiments LIGO and LISA we hope to see these innermost orbits and reconstruct a map of spacetime around black holes.

The instability of the innermost orbits around black holes will etch certain landmarks in a gravitational wave map. Gravitational waveforms of neighboring orbits will dechohere in a time scale set by the instability [10]. If the timescale for dissipation through gravitational radiation is faster than the instability timescale, then chaos will be damped and the gravitational wave signal will not observably decohere.

The simple set of unstable circular orbits around a Schwarzschild black hole are a consequence of the nonlinearity of general relativity. Their instability can be quantified by a positive Lyapunov exponent [10]. Although Lyapunov exponents are often associated with chaotic dynamics, the geodesics around a Schwarzschild black hole are not chaotic: the orbits are fully soluble and therefore integrable. However, under perturbation, chaos is likely to develop along the unstable circular and homoclinic orbits. An example of this has been found when the black holes spin. The nonlinearity degenerates to a nonintegrability and chaos [3–5]. The number of unstable periodic orbits proliferates so that they have to pack themselves into a fractal in order to crowd into that region of phase [7,5]. The unstable orbits will have positive Lyapunov exponents [11,12] and will emerge as fractals in phase space [4,5].

The Lyapunov exponents, while a seemingly useful tool, have uncomfortable shortcomings in the context of general relativity. Firstly, the Lyapunov exponents vary from orbit to orbit and so do not have the surveying power to scan the collective behaviour of all orbits that fractals methods do. Secondly, the Lyapunov exponents are a measure of the deviation of two neighboring orbits in time and therefore overtly depend on the time coordinate used. Since time is relative so too are the Lyapunov exponents. The relativity of the Lyapunov exponents has been known to erroneously lead to zero Lyapunov exponents for truly chaotic systems [13–16]. Importantly, topological measures of chaos such as fractals are coordinate invariant and are not plagued by the relativism of space and time [7,15].

In rare cases when there is a prefered time direction the ambiguity of time can be avoided. For the simplest case of a Schwarzschild black hole there is a timelike Killing vector which selects a prefered time direction. In other words, from our position asymptotically far away from the black hole, we use a well defined time coordinate in our observations. As long as we conscientiously compare all timescales in the same coordinate system, we should get meaningful comparisons.

We investigate the stability of three types of black hole binary: (i) Schwarzschild black hole (non-spinning, test particle motion), (ii) the Post-Newtonian (PN) expansion of the two-body problem (non-spinning black holes), and (iii) the chaotic orbits of spinning black holes in the PN-expansion.

The stability analysis begins with the equations of motion summarized as

$$\frac{dX_i}{dt} = H_i(X_j)\,. \tag{1.1}$$

To analyze the stability of a given orbit we linearize the equations of motion about that orbit

$$\frac{d\,\delta X_i(t)}{dt} = K_{ij}(t)\,\delta X_j(t)\,, \tag{1.2}$$

with

$$K_{ij}(t) = \left.\frac{\partial H_i}{\partial X_j}\right|_{X_i(t)} \tag{1.3}$$

the linear stability matrix. The solution to the linearized equations can be written as

$$\delta X_i(t) = L_{ij}(t)\,\delta X_j(0) \tag{1.4}$$

in terms of the evolution matrix which must obey

$$\dot{L}_{ij}(t) = K_{im} L_{mj}(t) \tag{1.5}$$

and $L_{ij}(0) = \delta_{ij}$. A determination of the eigenvalues of L_{ij} leads to the principal Lyapunov exponent. Specifically

$$\lambda = \lim_{t\to\infty} \frac{1}{t} \log\left(\frac{L_{jj}(t)}{L_{jj}(0)}\right)\,. \tag{1.6}$$

II. SCHWARZSCHILD ORBITS

A. Circular orbits

Here we evaluate the Lyapunov exponent of unstable orbits around the Schwarzschild black hole. We consider the usual geodesics of a non-spinning, light companion. We work in Schwarzschild time, the time measured by an observer asymptotically far from the black hole. The Lyapunov exponent was already evaluated in Ref. [10] in a different time coordinate system. This exemplifies the ambiguity of time. Still, the timescales which were compared in that paper were all measured in the same coordinate system and therefore the general conclusions of Ref. [10] still hold.

To isolate λ, we begin with the Lagrangian for a (non-spinning) test particle in the Schwarzschild spacetime

$$\mathcal{L} = \frac{1}{2}\left(-\frac{(r-2)}{r}\left(\frac{dt}{ds}\right)^2 + \frac{r}{r-2}\left(\frac{dr}{ds}\right)^2 + r^2\left(\frac{d\theta}{ds}\right)^2 + r^2\sin^2\theta\left(\frac{d\phi}{ds}\right)^2\right). \tag{2.1}$$

The black hole mass has been set to unity. We consider motion in an equatorial plane to eliminate the cylic θ variable by setting it equal to $\pi/2$ and define the canonical momenta by $\delta\mathcal{L}/\delta(dq/ds) = p_q$:

$$\begin{aligned} -p_t &= \frac{r-2}{r}\frac{dt}{ds} = E \\ p_\phi &= r^2\frac{d\phi}{ds} = L \\ p_r &= \frac{r}{r-2}\frac{dr}{ds}\,. \end{aligned} \tag{2.2}$$

To change into Schwarzschild time t, we use eqn. (2.2) to define the transformation

$$\frac{d}{ds} = \frac{Er}{r-2}\frac{d}{dt}\,. \tag{2.3}$$

Notice that in Ref. [10] an unusual time coordinate t' was used instead which was defined by the transformation

$$\frac{d}{ds} = \frac{r-2}{Er}\frac{d}{dt'}\,. \tag{2.4}$$

We will redo the stability analysis in Schwarzschild time t. The equations of motion can be derived through

$$\frac{\delta\mathcal{L}}{\delta dr/ds} - \frac{\delta\mathcal{L}}{\delta r} = 0 \tag{2.5}$$

and reduce to a two-dimensional system:

$$\begin{aligned} \dot{p}_r &= -\frac{E}{r(r-2)} - \frac{r-2}{r^3}\frac{p_r^2}{E} + \frac{r-2}{r^4}\frac{L^2}{E} \\ \dot{r} &= \left(\frac{r-2}{r}\right)^2\frac{p_r}{E} \end{aligned} \tag{2.6}$$

where an overdot denotes differentiation with respect to Schwarzschild time t. To compare with Ref. [10], we first consider circular orbits. Linearizing the equations of motion with $X_i(t) = (p_r, r)$ about orbits of constant r gives

$$K_{ij} = \begin{pmatrix} 0 & \frac{2(r-1)E}{r^2(r-2)^2} - \frac{L^2}{E}\frac{(3r-8)}{r^5} \\ \left(\frac{r-2}{r}\right)^2\frac{1}{E} & 0 \end{pmatrix} \tag{2.7}$$

The eigenvalues along circular orbits are

$$\lambda_\pm = \pm\left[\frac{2(r-1)}{r^4} - \frac{(3r-8)(r-2)^2}{r^7}\frac{L^2}{E^2}\right]^{1/2}\,. \tag{2.8}$$

For the unstable circular orbit at $r = 4$ the angular momentum and energy are $L = 4, E = 1$ respectively and the eigenvalues of K_{ij} are

$$\lambda_\pm = \pm\frac{1}{8\sqrt{2}}\,. \tag{2.9}$$

The conservation of energy ensures that in these canonical coordinates, the Lyapunov exponents must come in plus-minus pairs to conserve the volume of phase space.

The unit normalized eigenvectors corresponding to $\lambda_\pm$ are

$$\begin{aligned} \mathbf{e}_+ &= \frac{1}{3}\left(-1, 2\sqrt{2}\right) \\ \mathbf{e}_- &= \frac{1}{3}\left(1, 2\sqrt{2}\right)\,. \end{aligned} \tag{2.10}$$

In this eigenbasis K_{ij} is diagonal with

$$K_{ij} = \begin{pmatrix} \frac{1}{8\sqrt{2}} & 0 \\ 0 & -\frac{1}{8\sqrt{2}} \end{pmatrix} \tag{2.11}$$

so that

$$L_{ij} = \begin{pmatrix} \exp(\frac{1}{8\sqrt{2}}t) & 0 \\ 0 & \exp(-\frac{1}{8\sqrt{2}}t) \end{pmatrix} . \qquad (2.12)$$

Notice that in Ref. [10], the analysis was carried out in a four-dimensional coordinate system: $X_i' = (p_r, p_\phi, r, \phi)$. The additional coordinates are unimportant in the dynamical study and only hampered the diagonalization of K_{ij} [10]. If we were to redo the stability analysis in three coordinates $X'' = (p_r, p_\phi, r)$, we would get the same eigenvalues (2.9) and an additional $\lambda = 0$. If we move up to the four coordinates of X_i' we add yet another $\lambda = 0$ giving a degenerate set of eigenvalues. The matrix K_{ij} cannot be diagonalized in the event of degenerate eigenvalues which leads to an unnecessary complication. For this reason, we stick to the pertinent two-dimensional system $X_i = (p_r, r)$.

The relativity of time and the influence on the Lyapunov exponent is apparent at this stage. In Schwarschild time t we find $\lambda_\pm = \pm\frac{1}{8\sqrt{2}}$ while in the time t' used in Ref. [10], at $r = 4$ the exponents were found to be $\lambda'_\pm = \pm\frac{1}{2\sqrt{2}}$. The Lyapunov exponents are not coordinate invariant. However at $r = 4$, $t' = t/4$ and it follows that the combination

$$\lambda t = \lambda' t' \qquad (2.13)$$

is invariant.

We compare the Lyapunov timescale $T_\lambda = 1/\lambda$ to the gravitational wave timescale $T_w = 2\pi/\dot{\phi}$. For the orbit at $r = 4$, $T_\lambda/T_w = \sqrt{2}/\pi \approx 0.45$. The Lyapunov timescale is less than about one orbit around the central black hole. Notice that even though Ref. [10] operated in an unusual time, the calculations were performed self-consistently so that the ratio of T_λ to T_w is correct. The Lyapunov timescale is shorter than the gravitational wave timescale, making the instability observationally relevant.

In principle we could also compare T_λ to the decay time due to energy lost in the form of gravitational radiation. For a test-particle in a circular orbit around a Schwarzschild black hole the decay time is $T_d = (5/256)r^4/\mu$ where μ is the reduced mass. At $r = 4$ this is $T_d = 5/(3\mu) \gg 1$ since in the test-particle limit $\mu \ll 1$ and T_λ will be shorter than the decay time, again making the instability observationally relevant.

B. Homoclinic orbits

Although the unstable circular obits are often emphasized they are actually a subset of the pertinent orbits. The division between stability and instability for a Schwarzschild black hole is often taken to be the innermost stable circular orbit (ISCO). The ISCO is actually the saddle point at which the unstable circular orbit coincides with the stable circular orbit. From a dynamical systems point of view, the true division between stability and instability occurs more generally along the homoclinic orbits [1,2].

The stable manifold of a periodic orbit is defined as the set of points in phase space that, when evolved forwards in time, approach the periodic orbit. The unstable manifold is the set of points in phase that, when evolved backwards in time, approach the periodic orbit. For an integrable, nonchaotic system, the stable and unstable manifolds can intersect each other along a single orbit. This orbit is called homoclinic if it approaches the same fixed point in the past and in the future. For black holes the homoclinic orbits begin at an unstable circular orbit, roll out to a maximum radius and fall back in to the same unstable circular orbit. An example is shown in fig. 1. The homoclinic orbits are sometimes called zoom-and-whirl orbits in the gravitational wave literature because the orbits whirl around the center of mass and then zoom out into an ellipse before whirling in again.

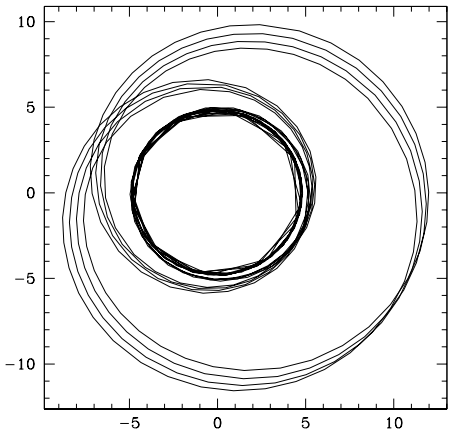

FIG. 1. A segment of the homoclinic orbit with $\beta = 1/4$.

Under perturbation the homoclinic orbits can become the site of a homoclinic tangle. The tangle occurs when the stable and unstable manifolds intersect transversely at an infinite number of points. The intersection will no longer occur along a simple line but will instead define a fractal set of chaotic orbits. In this section, we study the stability of the nonchaotic, simple set of homoclinic orbits around a Schwarzschild black hole. In §IV we study chaotic orbits of spinning black holes.

As is well known, orbital motion around a Schwarzschild black hole conveniently reduces to one-dimensional motion in an effective potential

$$\frac{1}{2}\dot{r}^2 + V_{\rm eff}(r) = E \qquad (2.14)$$

with

$$V_{\rm eff}(r) = E + \frac{(r-2)^3}{2E^2r^3}\left(1 + \frac{L^2}{r^2}\right) - \frac{(r-2)^2}{2r^2} . \qquad (2.15)$$

Circular orbits are solutions of $V_{\rm eff} = E$. For large enough angular momentum there are two circular orbits, one unstable and one stable. As found in Ref. [1], the homoclinic orbits have $E < 1$ and are described by the solution

$$p_r = \pm\frac{r}{r-2}\left[E^2 - \frac{r-2}{r}\left(1+\frac{L^2}{r^2}\right)\right]^{1/2}$$
$$\frac{1}{r} = \frac{1-2\beta}{6} + \frac{\beta}{2}\tanh^2(\sqrt{\beta}\phi/2) \tag{2.16}$$

where $0 \le \beta \le 1/2$ and $t(\phi)$ is a complicated function [1]. * The circular orbits can also be parameterzied by β as

$$r_{\rm unstable} = 6/(1+\beta)$$
$$r_{\rm stable} = 6/(1-\beta)$$
$$L = 2\sqrt{3/(1-\beta^2)}$$
$$E = \frac{2-\beta}{3}\sqrt{2/(1-\beta)}\,.$$

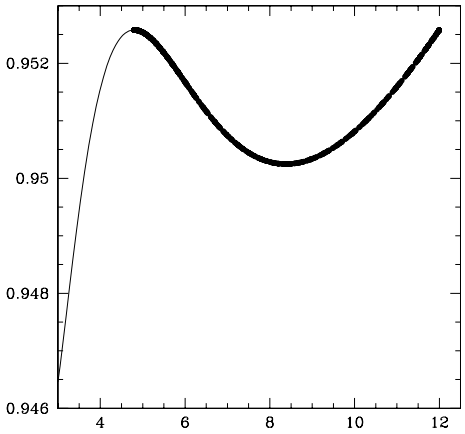

FIG. 2. The effective potential for orbits with $\beta = 1/4$. The segment in bold marks the corresponding homoclinic trajectory. The homoclinic orbit begins at the unstable circular orbit at the top of the hill ($r = 4.8$), rolls out past the stable circular orbit in the valley and on out to the maximum radius ($r = 12$) before rolling in again and climbing back up to the unstable orbit.

A homoclinic oribt starts at $r_{\rm unstable}$ and rolls out to

$$r_{\rm max} = 6/(1-2\beta) \tag{2.17}$$

winding around the black hole as it does so and then drops back in to $r_{\rm unstable}$. The ISCO is a homoclinic orbit with $\beta = 0$. The first homoclinic orbit at $\beta = 1/2$ starts at the unstable orbit at $r = 4$ and rolls out to infinity before returning. For $\beta = 1/4$, $r_{\rm unstable} = 4.8$, $r_{\rm stable} = 8$ and $r_{\rm max} = 12$. The effective potential for the homoclinic orbit is drawn in fig. 2. A segment of the orbit in the equatorial plane is represented in fig. 1.

To analyze the stability we linearize to find

$$K_{ij} = \begin{pmatrix} -\frac{2(r-2)}{r^3}\frac{p_r}{E} & \frac{2(r-1)E}{r^2(r-2)^2} + \frac{2(r-3)}{r^4}\frac{p_r^2}{E} - \frac{L^2}{E}\frac{(3r-8)}{r^5} \\ \left(\frac{r-2}{r}\right)^2\frac{1}{E} & \frac{4(r-2)}{r^3}\frac{p_r}{E} \end{pmatrix}. \tag{2.18}$$

The most general eigenvalues are

$$\ell_\pm = \left(\frac{r-2}{r^2}\right)\frac{p_r}{E} \pm \left[(2r-5)\frac{(r-2)^2}{r^6}\frac{p_r^2}{E^2} + 2\frac{(r-1)}{r^4} - \frac{(3r-8)(r-2)^2}{r^7}\frac{L^2}{E^2}\right]^{1/2} \tag{2.19}$$

Strictly speaking, ℓ is a stability exponent and is not identical to the time averaged Lyapunov exponent defined in eqn. (1.6). Figure 3 shows the real and imaginary parts of the positive stability exponent. As expected, the exponent is postive near the unstable inner radius and becomes imaginary in the vicinity of the stable circular radius dropping down to nearly zero as it reaches the apihelion and then runs back through these values as it moves back in to perihelion.

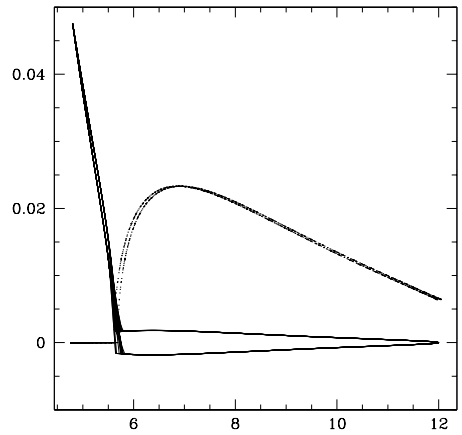

FIG. 3. $\beta = 1/4$ The solid line is the Real part of the positive stability exponent and the dotted line is the Imaginary part.

Because of this time variability in the stability along the orbit, we have to be cautious in interpreting the timescales. The gravitational wave frequency will jag up and down as the orbit zooms and whirls [2]. And it isn't obvious which timescales to compare. Instead of using the variable, analytic result we could try a time average.

To this end we compare the analytic value of ℓ from eqn. (2.19) to the time average Lyapunov exponent defined from eqn. (1.6)

*There appears to be typo in eqn. (1.5) of [2]. Eqn. (2.16) has a factor 1/2 which is missing from the second term in eqn. (1.5).

$$\lambda = \lim_{t\to\infty} \frac{1}{t} \log\left(\frac{L_{jj}(t)}{L_{jj}(0)}\right) . \tag{2.20}$$

For comparison we first look along the unstable circular orbit at $r = 4.8$. The upper panel of figure 4 shows the Lyapunov exponent as defined by eqn. (1.6) for the unstable circular orbit. The exponent was obtained by numerically integrating the L_{ij} using eqn. (1.5) and figure 4 shows λt versus t from eqn. (1.6). The numerically calculated value shown in figure 4 is identical to the analytic value given by eqn. (2.8) of $\lambda \approx 0.475$.

However for a homoclinic orbit which begins at $r = 4.8$, the time averaged (1.6) behaves as though there is no instability (lower panel of figure 4), when we know from the analytic result shown in fig. 3 that there is. The time averaged Lyapunov exponent will vanish along this orbit even though it clearly has an unstable segment. We have to be very cautious therefore when we interpret the Lyapunov exponent.

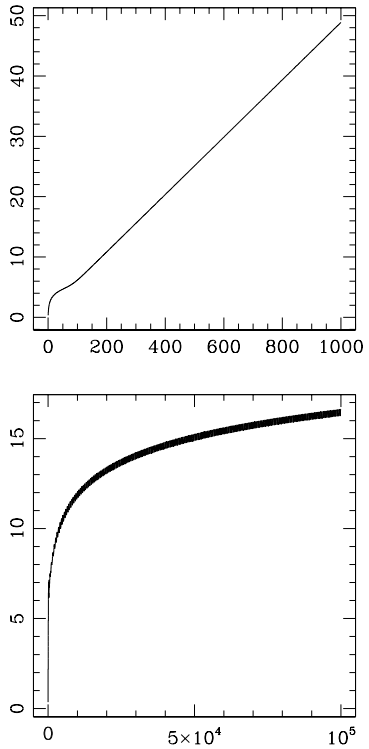

FIG. 4. $\beta = 1/4$. The slope of the line in the top panel is the numerically calculated Lyapunov exponent $\lambda \approx 0.475$ for the unstable circular orbit at $r = 4.8$ using eqn. (1.6). This matches exactly the analytic value predicted from eqn. (2.8). The slope of the line in the lower panel shows zero Lyapunov exponent as calculated by eqn. (1.6) for the homoclinic orbit. This is to be contrasted with the analytic value of the stability exponent shown in fig. 3 which has positive segments

For emphasis, if one was just scanning numerically, the mistaken conclusion could be drawn that these orbits were dynamically simple. This may turn out to be particularly important for the chaotic orbits of §IV.

III. POST-NEWTONIAN ORBITS

To move beyond the test particle limit, the two-body problem has been expanded in a Post-Newtonian (PN) expansion approximation to the fully relativistic two-body problem [17–19]. In this section we consider two black holes which are not spinning. In Ref. [2] the stability of the fixed points in the PN equations to second-order (2PN) was tested following [17]. We quote the results of Ref. [2] here. To second-order in the PN expansion, the center of mass equations of motion for the binary orbit can be written in harmonic coordinates as [17–19]

$$\ddot{r}_h = r_h\dot{\phi}^2 - \frac{1}{r_h^2}\left(A + B\dot{r}_h\right) \tag{3.1}$$

$$\ddot{\phi} = -\dot{\phi}\left(\frac{1}{r_h^2}B + 2\frac{\dot{r}_h}{r_h}\right) \tag{3.2}$$

where $M = 1$ is the total mass of the pair. The transformation between harmonic coordinates and Schwarzschild coordinates is $r_h = r - m$. The form of $A(r_h, \dot{r}_h, \dot{\phi})$ and $B(r_h, \dot{r}_h, \dot{\phi})$ depends on the relative masses of the two black holes and on the order of the PN expansion and can be found in Ref. [17].

As in Ref. [17], the stability of the fixed points is tested by perturbing eqns. (3.1)-(3.2) about a circular orbit to obtain,

$$K_{ij} = \begin{pmatrix} 0 & 1 & 0 \\ a & 0 & b \\ 0 & c & 0 \end{pmatrix} \tag{3.3}$$

with

$$\begin{aligned} a &= 3\dot{\phi}_o^2 - \frac{m}{r_{ho}^2}\left(\frac{\partial A}{\partial r_h}\right)_o \\ b &= 2r_{ho}\dot{\phi}_o - \frac{m}{r_{ho}^2}\left(\frac{\partial A}{\partial \dot{\phi}}\right)_o \\ c &= -\dot{\phi}_o\left(\frac{2}{r_{ho}} + \frac{m}{r_{ho}^2}\left(\frac{\partial B}{\partial \dot{r}_h}\right)_o\right) , \end{aligned} \tag{3.4}$$

where r_{ho} is the radius of the circular orbit in harmonic coordinates and $\dot{\phi}_o^2 = mA_o/r_{ho}^3$ is a function of the radius of the orbit and is found explicitly in Ref. [2]. The eigenvalues of (3.3) are,

$$\ell = 0, \quad \ell_\pm = \pm(a + bc)^{1/2} . \tag{3.5}$$

Stable oscillations about a circular orbit correspond to imaginary ℓ so that $a + bc < 0$. Unstable orbits correspond to real positive ℓ and so have $a + bc > 0$. The value of ℓ^2 for equal mass binaries as a function of the circular radius is plotted in fig. 5.

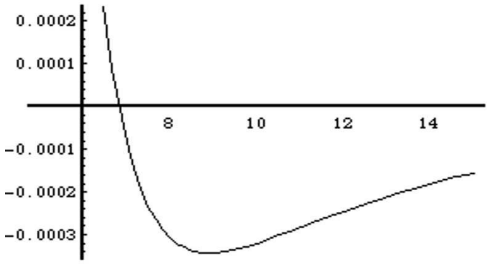

FIG. 5. ℓ^2 as a function of the constant circular radius in harmonic coordinates, r_{ho}. $\ell^2 > 0$ corresponds to unstable circular orbits and $\ell^2 < 0$ corresponds to stable circular orbits.

Using the results of Ref. [2] we deduce that in the test-mass limit, the innermost *unstable* circular orbit occurs at Schwarzschild radius $r_o = r_{ho} + 1 = 4.96$. A comparison to the gravitational wave timescale in the PN expansion then gives $T_\lambda/T_w \approx 0.158$. In the opposite extreme of equal mass binaries, the innermost *unstable* circular orbit occurs at $r_o = r_{ho}+1 = 5.78$ and $T_\lambda/T_w \approx 0.21$. A direct comparison to the Schwarzschild case isn't that valuable. What is noteworthy is that the Lyapunov timescales are again less than about one orbit around the center of mass. Consequently, one expects the decoherence of the gravitational waveform to be observationally significant. The instability timescales are comparable to the decay times although of course even a small loss in energy can induce merger for such an unstable orbit.

The analysis extended to homoclinic orbits can be gleaned from Ref. [2]. The homoclinic orbits to 2PN order show similar features to the homoclinic orbits of the Schwarzschild spacetime. The analytic Lyapunov exponent will pass from positive to imaginary values as the orbit winds around the center of mass. However, the time-averaged exponent will dilute these critical features.

None of these orbits are chaotic although they are unstable. We turn to the chaotic orbits of rapidly spinning binaries next.

IV. CHAOTIC ORBITS

The dynamics can become chaotic when the homoclinic orbit is perturbed leading to a homoclinic tangle. The intersection of the stable and unstable manifold will no longer occur along a line but will intersect transversally an infinite number of times. The fractal set of unstable chaotic orbits lies along this tangled intersection. Ref. [1] studied generic gravitational perturbations along the homoclinic orbits and found, as they expected, that the dynamics could become chaotic. The physical significance of the perturbations however wasn't clear and therefore the observational consequences were difficult to assess.

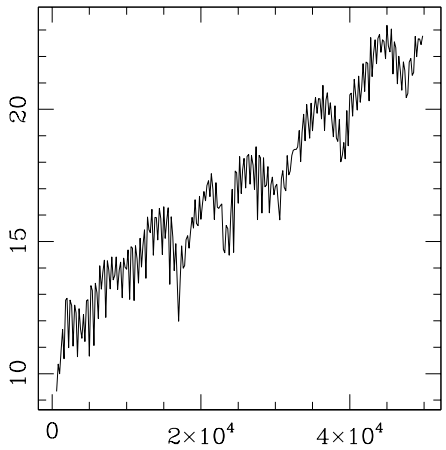

FIG. 6. The slope of the line is the Lyapunov exponent for the chaotic orbit of fig. 7.

The chaotic dynamics discovered in Ref. [3] for a supra-maximally spinning test-particle and for rapidly spinning pairs in the Post-Newtonian expansion [4,5], may occur along these homoclinic orbits. At the least the chaotic behaviour kicks up most conspicuously in the vicinity of these orbits.

We cannot determine the Lyapunov exponents analytically since the orbits are not analytically soluble - the very meaning of nonintegrability. We can however use eqn. (1.6) to numerically determine the exponents as we have done in Ref. [12]. The Lyapunov exponent for a maximally spinning pair of black holes is shown in fig. 6. The value read from this is $T_\lambda \approx 11$ in units of windings around the center of mass. A segment of the orbit projected onto a plane is shown in fig. 7.

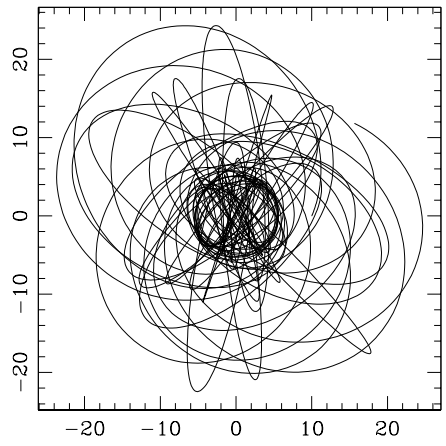

FIG. 7. A projection onto the plane of two maximally spinning black holes in a chaotic orbit.

For such an erratic orbit, it is not simple to define the gravitational wave timescale or the radiation reaction timescale. By starting the numerical simulation at a radius greater than 20 we found a rough estimate of

$T_d \sim 4-5$ orbits so that $T_\lambda/T_d > 2$ and the Lyapunov timescale is longer than the dissipation timescale. For this orbit the gravitational waveform will not have time to decohere before plunge and observations will not be severly disrupted by irregularity. However a factor of 2 is a tight margin especially since the PN-expansion is being pushed to extremes at such small separations.

It is important to stress that this is but one specific orbit and the ratio of T_λ/T_w will vary from orbit to orbit. Some chaotic orbits will undoubtedly have a longer Lyapunov timescale to dissipation timescale. A broad survey of the irregular region of phase space would be valuable. At 2PN order this is not so useful since the PN-expansion converges very slowly to the full relativistic problem. Notice for instance that T_λ is longer for this two-body approximation than it is for the fully relativistic Schwarzschild orbits. This may be a consequence of the slow convergence of the expansion and may show an underestimate of the instability. It is also possible that, like the homoclinic orbits, the measure of instability is diluted by the time average across the orbit. A survey at higher orders may be useful but requires a greater than 3PN-expansion that includes all spin arrangements and is not restricted to circular or quasi-circular orbits. We hope these higher orders will be available imminently and a survey of orbits will be viable in the near future.

SUMMARY

The Lyapunov exponents can be very useful for comparisons of physical scales. However, Lyapunov exponents also have some shortcomings which require we tread cautiously:

• Lyapunov exponents are relative. They depend on the worldline of the observer and the time they measure.

• They vary from orbit to orbit and may not contain generic information.

• They can give zero when averaged over orbits which move in and out of unstable regions.

Therefore, while important and useful, the Lyapunov exponents can be misleading and can only be used cautiously.

As far as we can trust them, the Lyapunov exponents give an estimate of the importance of instability to observations of gravitational waves. If the Lyapunov timescale is short compared to the inverse frequency of the gravitational waves emitted and is short compared to the dissipation timescale then instability will cause an observable decoherence of gravitational waves. We found that

• the Lyapunov timescale is shorter than both the gravitational wave timescale and the dissipation timescale for unstable circular orbits in the approximation of a test-particle around a Schwarzschild black hole,

• the Lyapunov timescale is shorter than the gravitational wave timesecale and comparable to the dissipation timescale for unstable circular orbits in the 2PN approximation in the absence of spins,

• and that the Lyapunov time was about a factor of 2 larger than the decay time for one randomly sampled chaotic orbit of a pair of maximally spinning black holes in the 2PN expansion.

The longer Lyapunov time for orbits in the 2PN approximation versus the test-particle approximation may be a real effect or it may be due to the slow convergence of the 2PN expansion to the full nonlinear problem or finally it may be due to the time average over such a varied orbit. In short, dissipation due to gravitational waves does abate chaos although the competition between chaos and dissipation is close. Better approximations to the two-body problem are needed to determine conclusively if chaos will affect observations of gravitational waves.

ACKNOWLEDGEMENTS

NJC is supported in part by National Science Foundation Grant No. PHY-0099532. JL is supported by a PPARC Advanced Fellowship and an award from NESTA.

[1] L.Bombelli and E.Calzetta, Class. Quantum. Grav. **9** 2573 (1992).
[2] J. Levin, R. O'Reilly, & E.J. Copeland, Phys. Rev. D**62**, 024023 (2000).
[3] S. Suzuki & K. Maeda, Phys. Rev. D**55**, 4848 (1997).
[4] J. Levin, Phys. Rev. Lett. **84**, 3515 (2000).
[5] J. Levin, gr-qc/0010100 (2001).
[6] G. Contopolous, Proc. R. Soc. **A431** 183 (1990); Proc. R. Soc. **A435** 551 (1990).
[7] C.P. Dettmann, N. E. Frankel & N.J. Cornish, Phys. Rev. D.**50** R618 (1994).
[8] N.J. Cornish and N.E.Frankel, Phys. Rev. D **56** 1903 (1997).
[9] J.Levin, Phys. Rev. D. **60** 64015 (1999).
[10] Neil J. Cornish, gr-qc/0206062.
[11] J.D. Schnittman & F.A. Rasio, Phys. Rev. Lett. **87**, 121101 (2001).
[12] N.J. Cornish and J. Levin, gr-qc/0207016; N.J. Cornish and J. Levin, gr-qc/0207020.
[13] J.D. Barrow, Phys. Rev. Lett. **46** 963 (1981); Phys. Rep. **85** 1 (1982).
[14] *Deterministic Chaos in General Relativity* eds. D. Hobill, A. Burd and A. Coley, (Plenum Press, New York, 1994) and references therein.
[15] N.J. Cornish & J.J. Levin, Phys. Rev. Lett. **78** 998 (1997); Phys. Rev. D.**55** 7489 (1997).
[16] See also, O. Semerak and V. Karas, Astron. Astrophys. 343 (1999) 325.

[17] L.E.Kidder, C.M.Will and A.G.Wiseman, Phys. Rev. D **47** 3281 (1993).
[18] C.W.Lincoln and C.M.Will, Phys. Rev. D. **42** 1123 (1990).
[19] T. Damour and N. Deruelle, C. R. Acad. Sci. Paris **293** 537 (1981); **293** 877 (1981).